The Journal of Infectious Diseases

MAJOR ARTICLE

Triggering Toll-Like Receptor 5 Signaling During Pneumococcal Superinfection Prevents the Selection of Antibiotic Resistance

Charlotte Costa,[1,a] Jean-Claude Sirard,[1,a] Paddy S. Gibson,[2] Jan-Willem Veening,[2] Erida Gjini,[3,a] and Mara Baldry[1,a]

[1]Univ. Lille, CNRS, Inserm, CHU Lille, Institut Pasteur de Lille, U1019 - UMR 9017 - CIIL - Center for Infection and Immunity of Lille, Lille, France; [2]Department of Fundamental Microbiology, Faculty of Biology and Medicine, University of Lausanne, Lausanne, Switzerland; and [3]Center for Computational and Stochastic Mathematics, Instituto Superior Técnico, Universidade de Lisboa, Lisbon, Portugal

Toll-like receptor 5 (TLR5) signaling plays a key role in antibacterial defenses. We previously showed that respiratory administration of flagellin, a potent TLR5 agonist, in combination with amoxicillin (AMX) improves the treatment of primary pneumonia or superinfection caused by AMX-sensitive or AMX-resistant *Streptococcus pneumoniae*. Here, the impact of adjunct flagellin therapy on antibiotic dose/regimen and the selection of antibiotic-resistant *S. pneumoniae* was investigated using superinfection with isogenic antibiotic-sensitive and antibiotic-resistant bacteria and population dynamics analysis. Our findings demonstrate that flagellin allows for a 200-fold reduction in the antibiotic dose, achieving the same therapeutic effect observed with antibiotic alone. Adjunct treatment also reduced the selection of antibiotic-resistant bacteria in contrast to the antibiotic monotherapy. A mathematical model was developed that captured the population dynamics and estimated a 20-fold enhancement immune-modulatory factor on bacterial clearance. This work paves the way for the development of host-directed therapy and refinement of treatment by modeling.

Keywords. flagellin; airways; antibiotic resistance; infection dynamics; modelling.

Lower respiratory tract infections are a major cause of death worldwide, contributing to more than 2 million deaths per year [1]. Among them, as a leading cause of disease and death, is pneumonia caused by viruses or bacteria [2]. *Streptococcus pneumoniae*, an opportunistic bacterium, is the main causative agent of community-acquired pneumonia and also capable of causing invasive disease, such as bacteremia or meningitis [3, 4]. The first-line treatment is amoxicillin (AMX), a β-lactam antibiotic. However, treatment failure is increasing due to the emergence of strains resistant to antibiotic [5]. Antibiotic resistance is now a major health concern, highlighting the need to develop new therapeutic strategies to overcome this burden.

Activation of innate immunity to effectively clear the bacteria is required during pneumococcal pneumonia [6, 7]. The airway innate immune response involves the activation of alveolar macrophages, epithelial cells, and neutrophils [8, 9]. Harnessing the power of innate immunity to overcome antibiotic-resistant infections, known as *host-directed therapy* or *immunotherapy,* is a promising alternative or adjunct to antibiotic therapy [10]. Targeting immunity to induce specific host antimicrobial defense mechanisms and modulate inflammation is of major interest, as multiple defenses are triggered by immunotherapies, and thus the development and selection of resistance is less likely compared with antimicrobial drugs. Moreover, immunotherapies are assumed to be efficient regardless of the drug resistance profile, the strain, the serotype, or the complexity of the infection (eg, coinfection or superinfection).

Toll-like receptors (TLRs) have been studied extensively as drug targets in immunotherapies [11, 12], as they are ubiquitously expressed and play a crucial role in sensing pathogens and generating immune responses [13]. Flagellin, the structural component of bacterial flagella, acts as a natural agonist for TLR5. Importantly, TLR5 is expressed on various cell types, including airway epithelial cells and immune cells [14]. The immunostimulatory activity of flagellin has been demonstrated

Received 26 January 2024; editorial decision 10 April 2024; accepted 07 May 2024; published online 8 May 2024

[a]C. C. and J. C. S. contributed equally to this work.

Correspondence: Jean-Claude Sirard, PhD, Institut Pasteur de Lille, Center for Infection and Immunity of Lille, 1 Rue du Pr Calmette, Lille Cedex 59019, France (jean-claude.sirard@inserm.fr); Erida Gjini, PhD, Department of Mathematics, Center for Computational and Stochastic Mathematics, Instituto Superior Técnico, Av Rovisco Pais, Lisbon 1049-001, Portugal (erida.gjini@tecnico.ulisboa.pt).

The Journal of Infectious Diseases® 2024;230:e1126–35

https://doi.org/10.1093/infdis/jiae239

in murine models of pneumococcal infection, whereby flagellin triggers the activation of local innate immune responses in a TLR5-dependent manner through signaling in the airway epithelium [15]. We have previously developed an adjunct immunotherapy to fight against pneumococcal pneumonia combining inhaled flagellin with the standard of care, AMX [16, 17]. The combination therapy has superior therapeutic effects compared with antibiotics alone, reducing bacterial load in the lungs, limiting systemic dissemination, and improving survival rates in murine models, even against antibiotic-resistant strains [17]. Whether immunotherapy is also effective at reducing selection of antibiotic resistance during infection is unknown.

Antibiotic resistance can occur by de novo mutations or horizontal gene transfer [18], such as with *S. pneumoniae,* which can exchange genetic material with other pneumococci and other species through natural transformation [19, 20]. Selecting for resistance traits within a bacterial population requires prolonged antibiotic pressure; otherwise the resistant population would be outcompeted due to the potential associated fitness costs. Misuse and overuse of antibiotics has greatly contributed to the acceleration of resistance selection. In 2019, a total of 1.27 million deaths were attributable to bacterial antimicrobial resistance [21].

As a means to examine selection dynamics over infection, mathematical modelling as a predictive tool for therapeutic outcome has gained momentum [22–26]. Theoretical studies have explored different treatment regimens—such as antibiotic dose, dosing frequency, and treatment duration—to establish criteria for effective infection clearance and prevention of resistance development, accounting in parallel for the contribution of host immune response [26, 27]. We hypothesized that the adjunct flagellin treatment to AMX can reduce the selection of AMX-resistant (AMX^R) bacteria during pneumococcal pneumonia by enhancing antibacterial immune defenses, ultimately leading to increased treatment efficacy. In the current study, we established a mouse coinfection model with AMX^R and AMX-sensitive (AMX^S) pneumococcal strains to analyze the dynamics of mixed pneumococcal population under immunotherapy. The data generated were then integrated within a mathematical model to predict treatment outcomes.

METHODS

Bacterial Strains and Cultures

S. pneumoniae strains are isogenic and derived from the serotype 2 laboratory strain D39V [28]. Genomic changes were introduced through transformation of linear polymerase chain reaction products followed by homologous recombination. Constructs were amplified from the *hlpA* locus of strains VL2678 [29] and VL2226 [30] with primers OVL43 (AACAAGTCAGCCACCTGTAG) and OVL46 (CGTGGCT GACGATAATGAGG). VL3198 is derived from AMX^R strain AMR53 (minimal inhibitory concentration [MIC], 2 µg/mL] [19], which was transformed with *hlpA::hlpA-mKate-ery*^{R} giving erythromycin resistance. VL3199 was cloned by inserting *hlpA::hlpA-gfp-chl*^{R} into D39V and as such is susceptible to AMX (MIC, 0.016 µg/mL) but resistant to chloramphenicol. For infection, working stocks were prepared as described elsewhere, in sterile Dulbecco's phosphate-buffered saline (PBS; Gibco) [15]. Bacterial numbers (as colony-forming units [CFUs]) were confirmed by plating serial dilutions onto 5% sheep blood agar plates and incubating at 37°C for 18 hours with 5% carbon dioxide.

Mouse Models of Infection

All experiments complied with institutional regulations and ethical guidelines, were approved by an Institutional Animal Care and Use Committee (E59-350009; Institut Pasteur de Lille; protocol APAFIS#16966 201805311410769_v3), and were conducted by qualified personnel. Male C57BL/6JRj mice (6–8 weeks old) (Janvier Laboratories) were maintained in ventilated cages (Innorack IVC Mouse 3.5) and handled in a laminar flow biosafety cabinet (class II biohazard configuration; Tecniplast). Before intranasal infection, the mice were anesthetized via intraperitoneal injection of 1.25 mg (50 mg/kg) of ketamine plus 0.25 mg (10 mg/kg) of xylazine in 250 µL of PBS. For the pneumococcal superinfection model, mice were sensitized by intranasal infection with 50 plaque-forming units of the murine-adapted H3N2 influenza A virus strain Scotland/20/74 in 30 µL of PBS. Seven days later, intranasal *S. pneumoniae* infection was induced with 5×10^4 CFUs in 30 µL of PBS [31, 32]. For coinfections, VL3199 and VL3198 bacteria were mixed at ratios of 1:1, 100:1, and 1000:1. At selected times, mice were euthanized via intraperitoneal injection of sodium pentobarbital (5.47 mg) in PBS (100 µL). Lungs were collected and homogenized with an UltraTurrax homogenizer (IKA-Werke), and viable bacterial counts were determined on blood agar plates containing selective antibiotic (erythromycin or chloramphenicol at 5 µg/mL; Sigma-Aldrich).

Flagellin and Antibiotic Administration

Flagellin (FLAMOD; recombinant flagellin $FliC_{\Delta 174–400}$ [33] harboring 1 extra amino acid at the N terminus) derives from *Salmonella enterica* serovar Typhimurium FliC and was produced in inclusion bodies in *Escherichia coli* by the Vaccine Development Department at Statens Serum Institut, Denmark. Flagellin was purified by filtration and chromatography and resuspended in 10 mmol/L phosphate, 145 mmol/L sodium chloride, polysorbate 80 (0.02% wt/vol; pH 6.5). Immunostimulatory activity was validated using the HEK-Dual hTLR5 cell assay (Invivogen). The endotoxin content in the protein preparation was assessed with a *Limulus* assay (Pyrochrome; kinetic LAL assay from Associates of Cape Cod). Flagellin

Table 1. Infection and Treatment Model Parameters

Parameter	Interpretation	Unit	Value
C	Within-host carrying capacity of bacteria	CFUs/lung	10^8
k	Half-saturation constant for immune stimulation	CFUs/lung	$10^{7.5}$
d	Inducible immunity-mediated clearance rate	h^{-1}(CFUs/lung)$^{-1}$	$10^{-6.5}$
δ	Static immune-mediated clearance rate	h^{-1}	0.72
h	Scaling parameter for the static immune response	(CFUs/lung)$^{-1}$	0.0005
σ	Inducible immunity activation rate	h^{-1}	0.1
r	Growth rate of sensitive bacteria	h^{-1}	Fitted: 0.33
c	Fitness cost of resistant bacteria	Constant ∈ (0, 1)	Fitted: 0.06
s	Antibiotic susceptibility factor of resistant bacteria	Constant ∈ (0, 1)	Fitted: 0.09
A_m	Maximal kill rate of antibiotic	h^{-1}	Fitted: 1.18
f	Immune-modulation factor of flagellin	Constant	Fitted: 20.1

Abbreviation: CFUs, colony-forming units.

(2.5 µg in 30 µL of PBS) was administrated intranasally under light anesthesia via isoflurane inhalation (Axience). Mice were treated intragastrically with AMX (5 µg to 1 mg of amoxicillin sodium [Clamoxyl, GlaxoSmithKline] in 200 µL of water). Control animals (mock-treated group) received intranasal PBS and/or intragastric water. Treatments always followed 12 hours after the pneumococcal infection.

Mathematical Modeling

The model was adapted from a previous theoretical study [27] and described the interplay between antibiotic-sensitive bacteria B_s, antibiotic-resistant bacteria B_r, inducible host immune defenses I, and the antibiotic treatment. The full structure and assumptions of the model are detailed in the Supplementary Materials (Supplement 1). Briefly, the infection dynamics in the lung were captured by the differential Equations 1–3:

$$\frac{dB_s}{dt} = rB_s\left(1-\frac{B}{C}\right) - dI\ B_s - \delta\frac{B_s}{1+hB} - A_mB_s\eta(t), \quad (1)$$

$$\frac{dB_r}{dt} = r(1-c)B_r\left(1-\frac{B}{C}\right) = dI\ B_r - \delta\frac{B_r}{1+hB} - sA_mB_r\eta(t), \quad (2)$$

and

$$\frac{dI}{dt} = \sigma I\frac{B}{B+k}, \quad (3)$$

where B is the total bacterial load (sum of B_s and B_r) and $\eta(t)$ is a step function between 0 and 1, denoting the time window of treatment between onset and the end of antibiotic therapy.

When flagellin was administered as adjunct with antibiotics, the inducible immunity-mediated clearance rate was modified as described by Equation 4:

$$d_{\text{flagellin}} = d(1+f\eta(t)). \quad (4)$$

Table 1 depicts the parameters definition and the associated values. The model parameters were established through a combination of theoretical considerations (as outlined in [27]), insights gained from the current experiments, and estimations detailed in the Supplementary Materials (Supplement 1), where the equations are fitted to the experiments. The experimental data used for model fitting comprise the dynamics of bacterial populations in response to infection and either no treatment (mock), AMX treatment (150 µg per animal), or AMX + flagellin adjunct treatment. The fitted data consist of 22 data points representing geometric means across several individuals (76 animals for a total of 152 values).

The parameters related to infection dynamics were shared across the treatments (Table 1). The parameter (A_m) associated with antibiotic effect was considered equal for the treatment scenarios AMX and AMX + flagellin, whereas the factor f that describes the immunomodulatory effect of flagellin was included only in the AMX + flagellin treatment. The model assumed that stimulation of immunity and immune-mediated clearance are symmetric for antibiotic-sensitive or antibiotic-resistant bacteria, whereas antibiotic-mediated clearance was defined higher for antibiotic-sensitive than for antibiotic-resistant bacteria. The initial conditions were fine-tuned based on the inoculum, considering the total CFU count and the relative densities of B_s and B_r. Nonlinear least-squares optimization was performed using MATLAB (MathWorks; version 9.13.0 [R2022b]; 2022) to find the best-fitting parameter values for the present data set, which minimize the sum of squared errors. Iterative fitting processes were conducted to derive confidence intervals and establish an uncertainty range for our predictions.

Statistical Analysis

The results were represented as geometric means. Intergroup differences were analyzed, using the Mann-Whitney test, 1-way analysis of variance Kruskal-Wallis test, and 2-way analysis of variance with uncorrected Fisher least significant difference post-test. All analyses were performed using Prism software (version 10.1.0; GraphPad Prism). Statistical significance was set to $P < .05$.

RESULTS

Respiratory Administration of Flagellin with Amoxicillin Increases Treatment Effectiveness of Pneumonia Caused by Amoxicillin-Sensitive and -Resistant *S. pneumoniae*

To determine the impact of flagellin adjunct therapy on the selection of antibiotic resistance during pneumonia, coinfection models were developed using a mixed bacterial population combining AMX^S (MIC, 0.016 μg/mL) and AMX^R *S. pneumoniae* (MIC, 2 μg/mL) (Figure 1*A*). The coinfection model was established in mice that were sensitized with influenza virus by intranasal infection 7 days before pneumococcal inoculation (ie, superinfection). After coinfection with AMX^S and AMX^R pneumococcal strains at a ratio of 1:1, mice were treated 12 hours later with a single intragastric administration of AMX or a combination of AMX with a single intranasal administration of flagellin. Two treatment doses of AMX were used: 5 μg (0.2 mg/kg) and 1 mg (40 mg/kg), a dose 200-fold higher. Based on previous pharmacokinetic data [34], serum AMX concentrations were expected to peak at 0.05 μg/mL for the 5 μg dose, corresponding to 3 × MIC for the AMX^S strain, and to 10 μg/mL for the 1 mg dose, corresponding to 5 × MIC for the AMX^R strain. Lung bacterial counts were determined 12 hours after treatment (Figure 1*B* and 1*C*).

Importantly, both strains had a similar fitness in mock treatment. Using the 5 μg AMX stand-alone regimen, the bacterial numbers of the AMX^S strain were 6-fold lower than in the mock group, whereas AMX^R bacterial numbers were not altered. When flagellin was administered with AMX, the bacterial counts were lower for both AMX^S and AMX^R strains compared with the mock condition (4000-fold and 10-fold lower, respectively). When a 1 mg dose of AMX was administered, the AMX^S population was fully cleared, while the AMX^R bacterial numbers were decreased 5-fold compared with the mock group and nearly eliminated by adjunct flagellin. Interestingly, the amounts of AMX^R bacteria in the animals treated with 5 μg AMX and flagellin or with 1 mg AMX alone were very similar, demonstrating that the combination of flagellin and AMX is equally effective as AMX used at a 200-fold higher dose. In conclusion, the adjunct immunotherapy with antibiotics adds value regardless of the antibiotic resistance profile and can reduce the antibiotic regimen and consequently decrease the selection of antibiotic-resistant bacteria.

Antibiotic Treatment Induces Selection of Amoxicillin-Resistant *S. pneumoniae*

We next investigated the effect of adjunct therapy on the selection of antibiotic resistance. To this end, a coinfection model was set up that mimics how antibiotic-resistant strains may be selected in vivo (Supplement 2—Supplementary Figure 1). Mice were superinfected with a 1000:1 ratio of AMX^S versus AMX^R *S. pneumoniae* (Figure 2*A*). A growth lag of 3 log was observed for the AMX^R strain in the absence of AMX (Figure 2*B*), which was overcome with AMX treatment (Figure 2*C*). While the amount of AMX^S bacteria was significantly higher than that of AMX^R in the mock-treated group, a single AMX administration was sufficient to promote the selection of antibiotic-resistant bacteria, which gained a competitive advantage over the sensitive population on treatment. Five treatments were required to completely eliminate AMX^S bacteria and significantly expand the AMX^R population. This pattern persisted for 24 hours after the last treatment, meaning that only a few days of antibiotic treatment were enough to durably select for antibiotic-resistant bacteria. In conclusion, this work established a model that resembles the clinically relevant selection of resistance during antibiotic therapy.

Adjunct Immunotherapy Treatment Delays and Reduces Antibiotic-Resistant Bacteria Selection

We next evaluated the effectiveness of flagellin immunotherapy in preventing the selection of antibiotic-resistant bacteria. Two consecutive administrations of AMX alone were sufficient to significantly select for growth and achieve the maximum lung carrying capacity of the resistant strain while reducing the number of AMX^S bacteria (Figure 3*A*). At 24 hours after infection, adjunct flagellin to AMX mostly abrogated the selection of AMX^R bacteria and highly reduced (by 3 log) the total bacteria in lungs compared with AMX treatment alone (Figure 3*B*). The resistant bacteria not cleared at 12 hours after treatment with AMX plus flagellin expanded to 10^4–10^5 CFUs per lung, but at lower levels than for AMX treatment alone (approximately 10^8 CFUs per lung), whereas the antibiotic-sensitive bacteria were totally cleared. These data show that flagellin immunotherapy not only delays but also significantly reduces resistance selection, in a time-dependent manner (Figure 3*C*). However, some mice responded poorly to the adjunct therapy, with resistant bacteria reaching 10^8 CFUs per lung, leading to death (33% non-responders). Despite these non-responders, the combination of AMX and flagellin showed improved therapeutic efficacy over antibiotic therapy alone and inhibited the selection of antibiotic resistant bacteria in vivo.

Modeling the Impact of Adjunct Therapy on Resistance Selection

To further quantify the outcome of treatments, we developed a mathematical model that characterizes the bacterial infection as follows: the pathogen grows, stimulates host immunity, and is ultimately controlled by immune responses, as described elsewhere [27] (Supplement 1—Supplementary Figure 1). The model considers that the infection is initiated by a mixture of the antibiotic-sensitive bacteria (B_s), which grow exponentially at a rate r, and antibiotic-resistant bacteria (B_r), which bear a fitness cost of resistance c, with both populations experiencing density-dependent limitation via a carrying capacity C (Equations 1–3 and Table 1). Varying 5 parameters, different

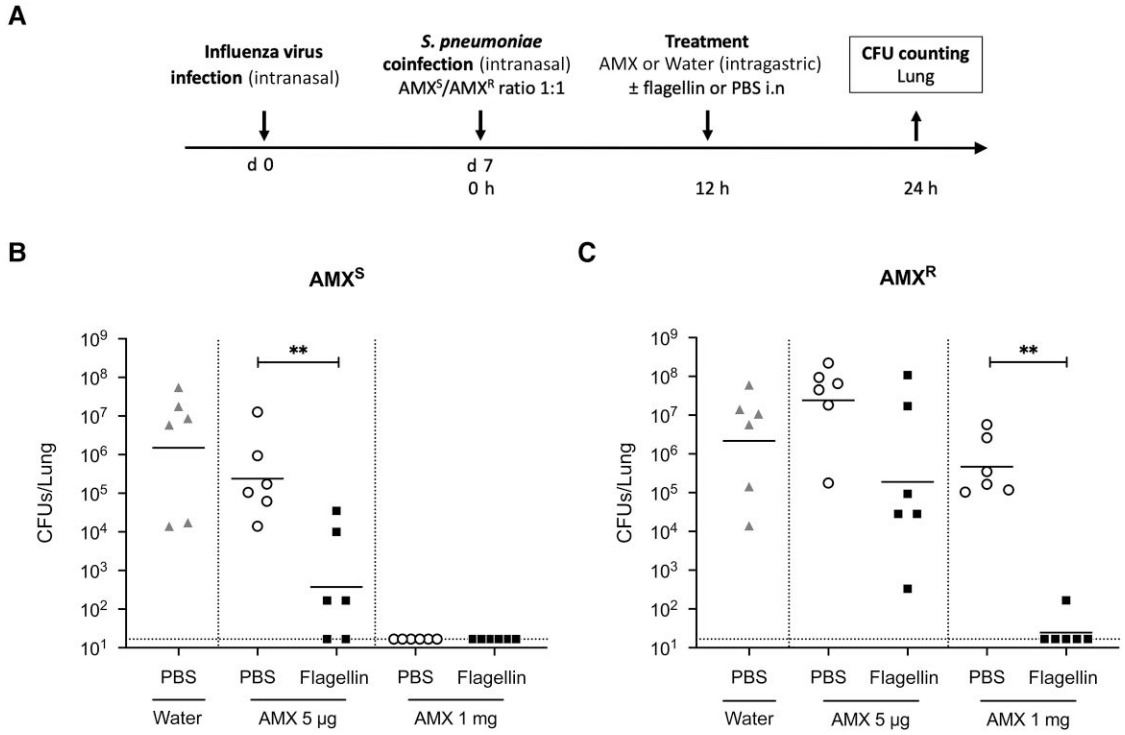

Figure 1. Efficacy of adjunct flagellin to amoxicillin (AMX) in a mouse coinfection with AMX-sensitive (AMX^S) and AMX-resistant (AMX^R) pneumococci. *A,* C57BL/6 mice (n = 6 per group) were infected intranasally with H3N2 virus, followed 7 days later by intranasal inoculation with 2.5×10^4 AMX^S and 2.5×10^4 AMX^R *Streptococcus pneumoniae* (1:1 ratio). Animals were treated 12 hours later by intragastric administration of AMX (5 µg or 1 mg) or water for the mock-treated group and intranasal administration of flagellin (2.5 µg) or phosphate-buffered saline (PBS). *B, C,* Lungs were collected 12 hours after treatment, and bacterial counts for AMX^S (*B*) and AMX^R strain (*C*) were determined. Symbols represent individual animals; solid lines, geometric mean values; and dashed lines, lower limits of detection. Data from PBS-treated and flagellin-treated mice were compared using the Mann-Whitney test; $^{**}P < .01$. Abbreviation: CFU, colony-forming unit.

values were tested through nonlinear optimization in MATLAB to determine the best-fitting combination for the experiments with adjunct therapy and antibiotic resistance selection (Figure 4 and Supplement 1—Supplementary Figures 2 and 3). The best-fitting model effectively captured the immediate post-treatment population dynamics and therapeutic outcomes, matching the observations in response to AMX or AMX + flagellin.

Notably, the model estimated a 20-fold (95% confidence interval, 19–29-fold) enhancement in the immunomodulatory effect of flagellin on the clearance rate of bacteria (Table 1 and Supplement 1—Supplementary Table 1), in line with the 3-log decrease in CFUs per lung observed in Figure 3. In addition, the model estimated a low fitness cost and a low antibiotic susceptibility factor for antibiotic-resistant bacteria ($c = 0.06$ *and* $s = 0.09$) and predicted that AMX treatment alone induces selection of high numbers of AMX^R bacteria, in line with the data (Figure 4). It was used to generate simulations of infection trajectories and to obtain and refine an uncertainty range for the model predictions (Supplement 1—Supplementary Figure 3). Some predictions indicated the possibility of a rebound of antibiotic-sensitive and antibiotic-resistant strains at later time points (ie, 84 hours after infection) but showed that when flagellin is administered in conjunction with AMX, this rebound is expected to occur later and at reduced levels compared with AMX alone. Moreover, we sought to refine the model to improve the fitting error sum of squared errors by extending the effect of AMX as well as the effect of flagellin beyond the 24 hour window. This model reduced the original error by 20%, suggesting the duration of therapeutic effect as an important avenue for further investigation (Supplement 1—Supplementary Figure 4). Thus, our mathematical model captures the lung infection population dynamics and therapeutic outcomes, highlighting the potential of adjunct flagellin treatment.

DISCUSSION

This study investigated the effect of respiratory administration of the activator of innate immunity flagellin in combination with AMX on the treatment efficacy against pneumococcal superinfection caused by mixed AMX^S and AMX^R *S. pneumoniae* infections. We have already shown that flagellin works in the context of primary and secondary pneumococcal infection (ie,

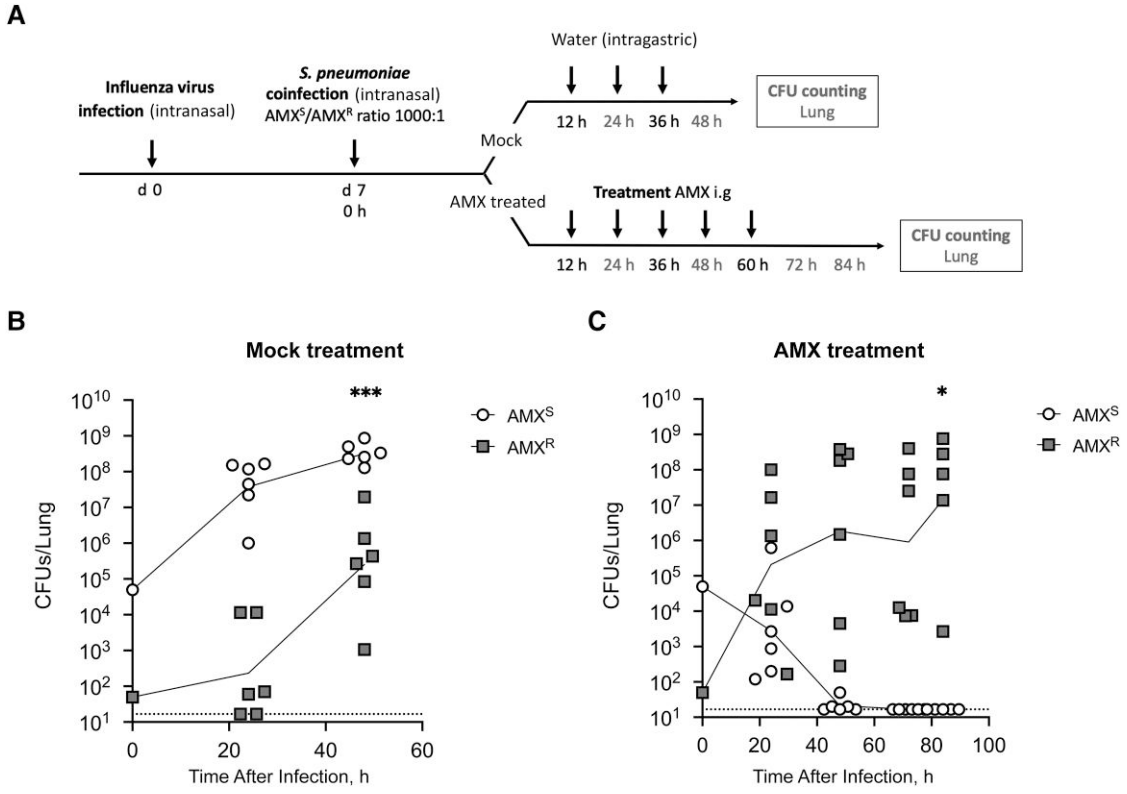

Figure 2. Selection of antibiotic-resistant bacteria in mice during antibiotic treatment. *A*, C57BL/6 mice (n = 6 per group) were infected intranasally with H3N2 virus, followed 7 days later by intranasal inoculation with 5×10^4 amoxicillin-sensitive (AMX^S) and 50 AMX-resistant (AMX^R) *Streptococcus pneumoniae* (1000:1 ratio). Animals were treated every 12 hours by intragastric administration of AMX (50 μg) or mock-treated with water. *B, C,* Lungs were collected 24, 48, 72, and 84 hours after infection, and bacterial counts of mock-treated (*B*) or AMX-treated mice (*C*) were performed. Symbols represent individual animals; solid lines, geometric mean values; and dashed lines, lower limits of detection. Two-way analysis of variance tests were applied to compare strains, time points and treatments: $^*P < .05$; $^{***}P < .001$. Abbreviation: CFU, colony-forming unit.

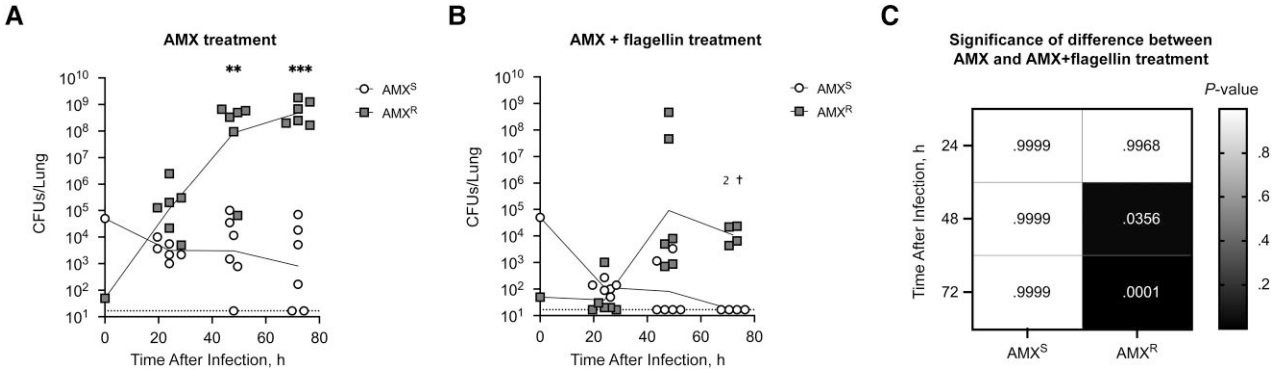

Figure 3. Reduced selection of antibiotic resistance with flagellin immunotherapy. C57BL/6 mice (n = 6 per group) were infected intranasally with H3N2 virus followed 7 days later by intranasal inoculation of 5×10^4 amoxicillin-sensitive (AMX^S) and 50 AMX-resistant (AMX^R) *Streptococcus pneumoniae* (1000:1 ratio). Animals were treated 12 hours later by a combination treatment: intragastric administration of AMX (150 μg) and intranasal administration of flagellin (2.5 μg) or phosphate-buffered saline (PBS), followed by a second administration of AMX at 24 hours. *A, B,* Lungs were collected 24, 48, and 72 hours after infection and bacterial counts of AMX-treated (*A*) or AMX + flagellin-treated (*B*) mice were performed. Symbols represent individual animals; solid lines, geometric mean values; dashed lines, lower limits of detection; cross, mice that died during the experiment due to the severity of the infection. Results are shown for a single experiment, representative of 2 experiments. Two-way analysis of variance tests were applied to compare strains, time points and treatments: $^{**}P < .01$; $^{***}P < .001$. *C*, Heat map representing significance of difference between AMX and AMX + flagellin treatments for each bacterial strain at each time point. Abbreviation: CFUs, colony-forming units.

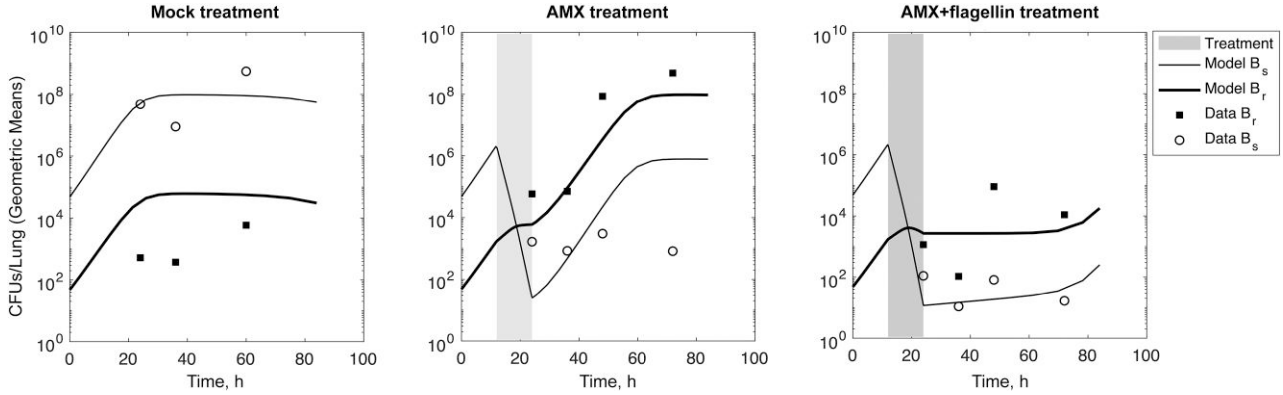

Figure 4. Modeling delayed antibiotic resistance selection after flagellin adjunct therapy. A mathematical model capturing infection dynamics has been tailored to experimental colony-forming unit (CFU) data on adjunct therapy and resistance selection, resulting in best-fitting parameter estimates. Lines and symbols depict, respectively, the best-fitting model predictions for each subpopulation (sum of squared errors, 0.37) and the experimental CFU geometric means; shaded regions, the window of treatment effect (ie, 12–24 hours). Abbreviations: AMX, amoxicillin; B_r, antibiotic-resistant bacteria; B_s, antibiotic-sensitive bacteria.

superinfection) models [16, 17], both of which are clinically relevant [35]. However, the effect of flagellin on antibiotic resistance selection remained to be evaluated. Addressing this, our results indicated that the addition of flagellin significantly reduced bacterial counts of both AMX^S and AMX^R strains compared to treatment with AMX alone, highlighting the potential of flagellin immunotherapy in combating antibiotic-resistant bacteria. Notably, the adjunct flagellin treatment displays effectiveness similar to that of the antibiotic used at a 200-fold higher dose. A coinfection model was established to mimic clinically relevant resistance selection during antibiotic therapy, revealing that antibiotic treatment promoted the selection and expansion of the resistant bacterial populations. However, adjunct flagellin treatment not only delayed but also reduced the selection of antibiotic-resistant bacteria. This suggests promising clinical applications for flagellin due to its capacity to reduce antibiotic dosage and to mitigate the selective pressure driving the emergence of antibiotic-resistant strains.

Boosters targeting innate immunity have shown efficacy against antibiotic-resistant strains [17, 36–39], yet their capacity to prevent the emergence of antibiotic resistance remains unclear. Studying de novo emergence of resistance through mutations in vivo poses significant challenges, primarily due to the associated fitness cost [40]. Here, an in vivo examination of antibiotic resistance selection was conducted, focusing on 2 strains characterized by antibiotic sensitivity and resistance. These strains demonstrated comparable fitness levels following successive rounds of mutations or acquisition of resistance via transformation [19, 40]. This innovative coinfection setup lays the foundation for future research on the effectiveness of treatments against antibiotic-resistant strains and the dynamics of these bacteria during pneumococcal pneumonia. A recent study reported the analysis of pneumococcal transformation in mice [41], highlighting the potential for exploring the effects of flagellin adjunct therapy of antibiotics on this mechanism, an essential driver of emergence.

As mathematical modelling offers an opportunity to quantify, predict and refine treatments, we integrated the data into a within-host model [27], incorporating bacterial coinfection with antibiotic-sensitive and antibiotic-resistant bacteria, natural immunity to infection, induction of innate immune response by flagellin, and antibiotic-mediated clearance. The model predicted better-controlled densities of AMX^S and AMX^R bacteria after treatment with the adjunct flagellin, through a mechanism of enhanced immune-mediated clearance (f factor), estimated in the range of 20-fold, and possible rebound later in the infection course. While theoretical frameworks offer a valuable tool for describing and assessing various regimens, they have their limitations [42]. For example, our mathematical model does not provide a mechanistic basis for the effect of flagellin but rather represents its net impact on enhanced bacterial clearance. Integrating features of more detailed models (eg, [43]) together with data on immune cell recruitment and immune mediator production would capture the mechanistic effect of flagellin.

Here we show that a single administration of flagellin proves insufficient for complete infection clearance. Porte et al [16] documented that 2–3 consecutive adjunct treatments of flagellin, coupled with AMX or trimethoprim-sulfamethoxazole, demonstrate efficacy against primary pneumococcal infections. However, whether similar outcomes can be expected in the context of selecting resistant bacterial clones during superinfection remains an area necessitating further investigations. Nevertheless, we know that mechanisms underlying antibacterial protection with adjunct treatment involve a combination of host effectors and antibiotics. Respiratory administration of flagellin is known to activate the TLR5-dependent lung innate immune defenses [44–47]. Studies in recent years demonstrated

superiority of the therapeutic effects of combined administration of AMX and a TLR4 immunomodulatory agonist during mouse *S. pneumoniae* infection, compared to AMX treatment [48, 49]. The enhanced protection was not only associated with TLR4-mediated boosting of immune defenses but also with modification of AMX pharmacokinetics, with a slower decline in the serum of AMX concentration. This suggests potential interactions between flagellin and antibiotic dynamics. Conversely, antibiotics may change the TLR5-dependent immune response dynamics. In our model, we have quantified parameters under assumption of a very short treatment window, but we see that the immune-modulation factor of flagellin (f) is sensitive to assumptions about the duration of therapeutic effect. A comprehensive integration of the pharmacokinetic attributes of flagellin and antibiotic will be essential to further map dosing administration details to infection resolution parameters and develop adjunct treatments.

In conclusion, the therapeutic potential of adjunct treatment extends beyond the standard of care antibiotics, as it surpasses the cumulative value of the individual components administered separately. This evidence strengthens the argument for the importance of investigating and modelling the mechanisms responsible for the remarkable efficacy of the flagellin-antibiotic combination.

Supplementary Data

Supplementary materials are available at *The Journal of Infectious Diseases* online (http://jid.oxfordjournals.org/). Supplementary materials consist of data provided by the author that are published to benefit the reader. The posted materials are not copyedited. The contents of all supplementary data are the sole responsibility of the authors. Questions or messages regarding errors should be addressed to the author.

Notes

Acknowledgments. We thank the Vaccine Development Department of Statens Serum Institut (Denmark) for the manufacture and supply of FLAMOD (flagellin) and the animal core facilities of the Univ. Lille, CNRS, Inserm, CHU Lille, Institut Pasteur de Lille, US 41–UAR 2014–PLBS, Lille, for technical assistance.

Author contributions. C. C., J. C. S., P. S. G., E. G., and M. B. planned studies, performed experiments, and analyzed data. C. C., J. C. S., J. W. V., E. G., and M. B. wrote the manuscript. J. C. S. and M. B. supervised the project.

Financial support. The study was funded by Institut National de la Santé et de la Recherche Médicale (Inserm); Institut Pasteur de Lille; Université de Lille; the project FAIR, which received funding from the European Union's Horizon 2020 research and innovation program (under grant agreement 847786); the Swiss National Science Foundation (SNSF) (grants 310030_192517, 310030_200792, and 51NF40_180541 supporting work in J. W. V.'s laboratory); and the Portuguese Foundation for Science and Technology (grant CEECIND/03051/2018 to E. G.).

Potential conflicts of interest. J. C. S. is the inventor of the patents WO2009156405, WO2011161491, and WO2015011254, which describes the use of the recombinant flagellin in this study as an adjunct of antibiotics. All other authors report no potential conflicts.

All authors have submitted the ICMJE Form for Disclosure of Potential Conflicts of Interest. Conflicts that the editors consider relevant to the content of the manuscript have been disclosed.

References

1. GBD 2016 Lower Respiratory Infections Collaborators. Estimates of the global, regional, and national morbidity, mortality, and aetiologies of lower respiratory infections in 195 countries, 1990–2016: a systematic analysis for the global burden of disease study 2016. Lancet Infect Dis **2018**; 18:1191–210.
2. Ieven M, Coenen S, Loens K, et al. Aetiology of lower respiratory tract infection in adults in primary care: a prospective study in 11 European countries. Clin Microbiol Infect **2018**; 24:1158–63.
3. van der Poll T, Opal SM. Pathogenesis, treatment, and prevention of pneumococcal pneumonia. Lancet **2009**; 374: 1543–56.
4. Weiser JN, Ferreira DM, Paton JC. *Streptococcus pneumoniae*: transmission, colonization and invasion. Nat Rev Microbiol **2018**; 16:355–67.
5. Yahiaoui RY, den Heijer C, van Bijnen EM, et al. Prevalence and antibiotic resistance of commensal *Streptococcus pneumoniae* in nine European countries. Future Microbiol **2016**; 11:737–44.
6. Kadioglu A, Andrew PW. The innate immune response to pneumococcal lung infection: the untold story. Trends Immunol **2004**; 25:143–9.
7. von Bernuth H, Picard C, Jin Z, et al. Pyogenic bacterial infections in humans with MyD88 deficiency. Science **2008**; 321:691–6.
8. Yamamoto K, Ahyi AN, Pepper-Cunningham ZA, et al. Roles of lung epithelium in neutrophil recruitment during pneumococcal pneumonia. Am J Respir Cell Mol Biol **2014**; 50:253–62.
9. Famà A, Midiri A, Mancuso G, et al. Nucleic acid-sensing Toll-like receptors play a dominant role in innate immune recognition of pneumococci. mBio **2020**; 11:e00415-20.
10. Wallis RS, O'Garra A, Sher A, Wack A. Host-directed immunotherapy of viral and bacterial infections: past, present and future. Nat Rev Immunol **2023**; 23:121–33.
11. Tan AC, Mifsud EJ, Zeng W, et al. Intranasal administration of the TLR2 agonist Pam2Cys provides rapid protection against influenza in mice. Mol Pharm **2012**; 9:2710–8.

12. Fensterheim BA, Young JD, Luan L, et al. The TLR4 agonist monophosphoryl lipid A drives broad resistance to infection via dynamic reprogramming of macrophage metabolism. J Immunol **2018**; 200:3777–89.
13. Vijay K. Toll-like receptors in immunity and inflammatory diseases: past, present, and future. Int Immunopharmacol **2018**; 59:391–412.
14. Vijayan A, Rumbo M, Carnoy C, Sirard JC. Compartmentalized antimicrobial defenses in response to flagellin. Trends Microbiol **2018**; 26:423–35.
15. Muñoz N, Van Maele L, Marqués JM, Rial A, Sirard JC, Chabalgoity JA. Mucosal administration of flagellin protects mice from *Streptococcus pneumoniae* lung infection. Infect Immun **2010**; 78:4226–33.
16. Porte R, Fougeron D, Muñoz-Wolf N, et al. A Toll-like receptor 5 agonist improves the efficacy of antibiotics in treatment of primary and influenza virus-associated pneumococcal mouse infections. Antimicrob Agents Chemother **2015**; 59:6064–72.
17. Matarazzo L, Casilag F, Porte R, et al. Therapeutic synergy between antibiotics and pulmonary Toll-like receptor 5 stimulation in antibiotic-sensitive or -resistant pneumonia. Front Immunol **2019**; 10:723.
18. Bengtsson-Palme J, Kristiansson E, Larsson DGJ. Environmental factors influencing the development and spread of antibiotic resistance. FEMS Microbiol Rev **2018**; 42:fux053.
19. Gibson PS, Bexkens E, Zuber S, Cowley LA, Veening JW. The acquisition of clinically relevant amoxicillin resistance in *Streptococcus pneumoniae* requires ordered horizontal gene transfer of four loci. PLoS Pathog **2022**; 18:e1010727.
20. Salvadori G, Junges R, Morrison DA, Petersen FC. Competence in *Streptococcus pneumoniae* and close commensal relatives: mechanisms and implications. Front Cell Infect Microbiol **2019**; 9:94.
21. Antimicrobial Resistance Collaborators. Global burden of bacterial antimicrobial resistance in 2019: a systematic analysis. Lancet **2022**; 399:629–55.
22. Day T, Read AF. Does high-dose antimicrobial chemotherapy prevent the evolution of resistance? PLoS Comput Biol **2016**; 12:e1004689.
23. Handel A, Margolis E, Levin BR. Exploring the role of the immune response in preventing antibiotic resistance. J Theor Biol **2009**; 256:655–62.
24. Geli P, Laxminarayan R, Dunne M, Smith DL. "One-size-fits-all"? optimizing treatment duration for bacterial infections. PLoS One **2012**; 7:e29838.
25. Gjini E, Brito PH. Integrating antimicrobial therapy with host immunity to fight drug-resistant infections: classical vs. adaptive treatment. PLoS Comput Biol **2016**; 12: e1004857.
26. Ankomah P, Levin BR. Exploring the collaboration between antibiotics and the immune response in the treatment of acute, self-limiting infections. Proc Natl Acad Sci U S A **2014**; 111:8331–8.
27. Gjini E, Paupério FFS, Ganusov VV. Treatment timing shifts the benefits of short and long antibiotic treatment over infection. Evol Med Public Health **2020**; 2020:249–63.
28. Slager J, Aprianto R, Veening JW. Deep genome annotation of the opportunistic human pathogen *Streptococcus pneumoniae* D39. Nucleic Acids Res **2018**; 46:9971–89.
29. Kurushima J, Campo N, van Raaphorst R, Cerckel G, Polard P, Veening JW. Unbiased homeologous recombination during pneumococcal transformation allows for multiple chromosomal integration events. Elife **2020**; 9:e58771.
30. Kjos M, Veening JW. Tracking of chromosome dynamics in live *Streptococcus pneumoniae* reveals that transcription promotes chromosome segregation. Mol Microbiol **2014**; 91:1088–105.
31. De Santo C, Arscott R, Booth S, et al. Invariant NKT cells modulate the suppressive activity of IL-10-secreting neutrophils differentiated with serum amyloid A. Nat Immunol **2010**; 11:1039–46.
32. Paget C, Ivanov S, Fontaine J, et al. Potential role of invariant NKT cells in the control of pulmonary inflammation and $CD8^+$ T cell response during acute influenza A virus H3N2 pneumonia. J Immunol **2011**; 186:5590–602.
33. Nempont C, Cayet D, Rumbo M, Bompard C, Villeret V, Sirard JC. Deletion of flagellin's hypervariable region abrogates antibody-mediated neutralization and systemic activation of TLR5-dependent immunity. J Immunol **2008**; 181:2036–43.
34. Mondemé M, Zeroual Y, Soulard D, et al. Amoxicillin treatment of pneumococcal pneumonia impacts bone marrow neutrophil maturation and function. J Leukoc Biol **2024**; 115:463–75.
35. Morens DM, Taubenberger JK, Fauci AS. Predominant role of bacterial pneumonia as a cause of death in pandemic influenza: implications for pandemic influenza preparedness. J Infect Dis **2008**; 198:962–70.
36. Kinnebrew MA, Ubeda C, Zenewicz LA, Smith N, Flavell RA, Pamer EG. Bacterial flagellin stimulates Toll-like receptor 5–dependent defense against vancomycin-resistant *Enterococcus* infection. J Infect Dis **2010**; 201:534–43.
37. Abt MC, Buffie CG, Sušac B, et al. TLR-7 activation enhances IL-22-mediated colonization resistance against vancomycin-resistant *Enterococcus*. Sci Transl Med **2016**; 8:327ra25.
38. Lee YJ, Kim JK, Jung CH, et al. Chemical modulation of SQSTM1/p62-mediated xenophagy that targets a broad range of pathogenic bacteria. Autophagy **2022**; 18:2926–45.

39. Alphonse MP, Rubens JH, Ortines RV, et al. Pan-caspase inhibition as a potential host-directed immunotherapy against MRSA and other bacterial skin infections. Sci Transl Med **2021**; 13:eabe9887.
40. Nishimoto AT, Dao TH, Jia Q, et al. Interspecies recombination, not de novo mutation, maintains virulence after β-lactam resistance acquisition in *Streptococcus pneumoniae*. Cell Rep **2022**; 41:111835.
41. Echlin H, Iverson A, Sardo U, Rosch JW. Airway proteolytic control of pneumococcal competence. PLoS Pathog **2023**; 19:e1011421.
42. Krakauer DC, Collins JP, Erwin D, et al. The challenges and scope of theoretical biology. J Theor Biol **2011**; 276: 269–76.
43. Domínguez-Hüttinger E, Boon NJ, Clarke TB, Tanaka RJ. Mathematical modeling of *Streptococcus pneumoniae* colonization, invasive infection and treatment. Front Physiol **2017**; 8:115.
44. Van Maele L, Fougeron D, Janot L, et al. Airway structural cells regulate TLR5-mediated mucosal adjuvant activity. Mucosal Immunol **2014**; 7:489–500.
45. Fougeron D, Van Maele L, Songhet P, et al. Indirect Toll-like receptor 5-mediated activation of conventional dendritic cells promotes the mucosal adjuvant activity of flagellin in the respiratory tract. Vaccine **2015**; 33:3331–41.
46. Yu FS, Cornicelli MD, Kovach MA, et al. Flagellin stimulates protective lung mucosal immunity: role of cathelicidin-related antimicrobial peptide. J Immunol **2010**; 185:1142–9.
47. Janot L, Sirard JC, Secher T, et al. Radioresistant cells expressing TLR5 control the respiratory epithelium's innate immune responses to flagellin. Eur J Immunol **2009**; 39: 1587–96.
48. Franck S, Fuhrmann-Selter T, Joseph JF, et al. A rapid, simple and sensitive liquid chromatography tandem mass spectrometry assay to determine amoxicillin concentrations in biological matrix of little volume. Talanta **2019**; 201:253–8.
49. Casilag F, Matarazzo L, Franck S, et al. The biosynthetic monophosphoryl lipid A enhances the therapeutic outcome of antibiotic therapy in pneumococcal pneumonia. ACS Infect Dis **2021**; 7:2164–75.